v-SNARE cellubrevin is required for basolateral sorting of AP-1B–dependent cargo in polarized epithelial cells

Ian C. Fields,[1] Elina Shteyn,[1] Marc Pypaert,[2] Véronique Proux-Gillardeaux,[3] Richard S. Kang,[1] Thierry Galli,[3] and Heike Fölsch[1]

[1]Department of Biochemistry, Molecular Biology and Cell Biology, Northwestern University, Evanston, IL 60208
[2]Department of Cell Biology, Yale University School of Medicine, New Haven, CT 06520
[3]Institut National de la Santé et de la Recherche Médicale Avenir Team, Institut Jacques Monod, Unité Mixte de Recherche 7592, Centre National de la Recherche Scientifique, Universities Paris 6 and Paris 7, F-75005 Paris, Cedex 05, France

The epithelial cell–specific adaptor complex AP-1B is crucial for correct delivery of many transmembrane proteins from recycling endosomes to the basolateral plasma membrane. Subsequently, membrane fusion is dependent on the formation of complexes between SNARE proteins located at the target membrane and on transport vesicles. Although the t-SNARE syntaxin 4 has been localized to the basolateral membrane, the v-SNARE operative in the AP-1B pathway remained unknown. We show that the ubiquitously expressed v-SNARE cellubrevin localizes to the basolateral membrane and to recycling endosomes, where it colocalizes with AP-1B. Furthermore, we demonstrate that cellubrevin coimmunoprecipitates preferentially with syntaxin 4, implicating this v-SNARE in basolateral fusion events. Cleavage of cellubrevin with tetanus neurotoxin (TeNT) results in scattering of AP-1B localization and missorting of AP-1B–dependent cargos, such as transferrin receptor and a truncated low-density lipoprotein receptor, LDLR-CT27. These data suggest that cellubrevin and AP-1B cooperate in basolateral membrane trafficking.

Introduction

During embryonic development, columnar epithelial cells polarize their plasma membrane into distinct apical and basolateral domains that are separated by tight junctions. Once established, this polarity has to be maintained, and it has to be ensured that apical and basolateral transmembrane proteins are correctly sorted to the respective target domain (Mostov et al., 2003; Nelson, 2003).

Frequently, a first step in basolateral sorting is the recognition of a targeting determinant encoded in the cytoplasmic tail of transmembrane proteins. Perhaps the best-characterized sorting determinants are similar to endocytosis signals and consist of either LL- or Y-based sorting signals. These basolateral signals are in general cis-dominant over apical sorting information such as *N*- or *O*-glycosylations in a protein's ectodomain (Schuck and Simons, 2004). Although it is still unclear how proteins with LL-based sorting signals are selected for basolateral delivery, a better understanding has been achieved for the Y-based sorting signals (Rodriguez-Boulan et al., 2005). Typically, Y-based sorting signals are recognized by the medium subunits of heterotetrameric clathrin adaptor protein (AP) complexes (Nakatsu and Ohno, 2003). There are four major types, AP-1 through AP-4, all sharing the same general subunit organization with two large subunits (γ, α, δ, ε, and β1–β4), one medium subunit (μ1–μ4), and one small subunit (σ1–σ4; Boehm and Bonifacino, 2001). Although AP-1, AP-3, and AP-4 are all thought to mediate cargo selection and vesicle formation at the TGN or endosomes, AP-2 is involved in clathrin-mediated endocytosis (Brodsky et al., 2001; Robinson and Bonifacino, 2001). Most polarized epithelial cells actually contain two highly similar AP-1 complexes, the ubiquitously expressed AP-1A, thought to mediate endosomal sorting, and the epithelial-specific AP-1B complex involved in basolateral targeting (Fölsch et al., 1999). AP-1A and AP-1B differ only in the incorporation of their medium subunits μ1A or μ1B, respectively. Despite this close homology, AP-1A and AP-1B have largely

Correspondence to Heike Fölsch: h-folsch@northwestern.edu

Abbreviations used in this paper: AP, adaptor protein; FcR, FcII-B2 receptor; LDLR, low-density lipoprotein receptor; TeNT, tetanus neurotoxin; TfnR, transferrin receptor; VAMP, vesicle-associated membrane protein; VSVG, vesicular stomatitis virus glycoprotein.

The online version of this article contains supplemental material.

The Journal of Cell Biology, Vol. 177, No. 3, May 7, 2007 477–488
http://www.jcb.org/cgi/doi/10.1083/jcb.200610047

nonoverlapping functions and form distinct vesicle populations (Fölsch et al., 2001, 2003). The different roles of AP-1A and AP-1B in sorting can partially be explained by their differential localization to the TGN and recycling endosomes, respectively (Gan et al., 2002; Fölsch et al., 2003).

Besides AP-1B, the only other adaptor complex implicated in basolateral sorting is AP-4 (Simmen et al., 2002). Although AP-4 is thought to mediate basolateral sorting at the TGN, AP-1B is involved in recycling internalized cargo back from recycling endosomes to the basolateral membrane. In addition, AP-1B may also regulate basolateral delivery of newly synthesized proteins, which may travel through recycling endosomes on their way to the plasma membrane (Ang et al., 2003, 2004; Fölsch, 2005). Despite the clear advances in our understanding of adaptor complexes involved, little is known about the relationship of sorting basolateral cargo at the TGN or the recycling endosomes (e.g., to what extent does biosynthetic cargo move through recycling endosomes?), and the interaction of specific basolateral sorting determinants with the individual μ-chains has not been established; however, the latter information would add considerably to our mechanistic understanding of basolateral sorting pathways.

Regardless, once the basolateral transport vesicles are formed, tethering to and fusion with the correct target site has to be ensured. The mammalian exocyst, an eight-subunit complex, is thought to facilitate tethering of basolateral vesicles with the target site, and at least two of its subunits associate with AP-1B vesicles (Grindstaff et al., 1998; Fölsch et al., 2003). After tethering, the complex may rearrange to bring vesicle and plasma membrane into close contact to allow for SNARE pairing and subsequent fusion (Munson and Novick, 2006). SNAREs are soluble NSF attachment protein receptors. Plasma membrane SNAREs of the syntaxin family (e.g., syntaxins 1, 2, 3, and 4) and the synaptosomal-associated protein of 23 kD (SNAP-23) form the so-called target SNAREs (t-SNAREs) that, upon interaction with the vesicle-associated membrane proteins (VAMPs/v-SNAREs), mediate the exocytic fusion reaction (Ravichandran et al., 1996; Bonifacino and Glick, 2004; Jahn and Scheller, 2006).

Epithelial cells express three different t-SNAREs at the plasma membrane. Syntaxin 3 localizes to the apical domain, syntaxin 4 is basolateral, and syntaxin 2 in renal epithelial cells localizes either to the apical or basolateral membrane, whereas exogenously expressed syntaxin 2 in MDCK cells is nonpolarized (Low et al., 1996; Li et al., 2002). Recently, it has been shown that the correct localization of syntaxin 3 is necessary for epithelial polarity and correct targeting of proteins to the apical membrane (Kreitzer et al., 2003; ter Beest et al., 2005; Sharma et al., 2006). The role of syntaxin 4 in basolateral sorting is suspected but has not yet been demonstrated. Furthermore, the nature of the corresponding v-SNARE is still elusive. It has been shown that the addition of tetanus neurotoxin (TeNT) to permeabilized MDCK cells slowed the transport rate of vesicular stomatitis virus glycoprotein (VSVG) to the basolateral domain but not the transport of influenza HA to the apical domain (Ikonen et al., 1995). Apical targeting was then shown to involve the TeNT-resistant v-SNARE TI-VAMP (VAMP7) and syntaxin 3–dependent fusion (Galli et al., 1998; Low et al., 1998; Lafont et al., 1999). However, the exact nature of the SNARE proteins involved in basolateral targeting was not determined, and it remains to be shown whether treatment with TeNT results in any sorting defects to the basolateral domain.

TeNT is a highly specific clostridial neurotoxin that has three known targets: synaptobrevin 1 (VAMP 1), synaptobrevin 2 (VAMP 2), and cellubrevin (VAMP 3; Yamasaki et al., 1994). Although synaptobrevin 1 is mainly brain specific, synaptobrevin 2 has a broader expression profile, including adipocytes and exocrine tissues (Ralston et al., 1994; Rossetto et al., 1996). In contrast, cellubrevin is ubiquitously expressed and has been shown to play a role in epithelial cell migration (McMahon et al., 1993; Proux-Gillardeaux et al., 2005). Furthermore, cellubrevin has been implicated in recycling of transferrin receptors (TfnRs) in fibroblasts and apical recycling pathways in MDCK cells (Galli et al., 1994; Daro et al., 1996; Steegmaier et al., 2000). However, because apical targeting was shown to be resistant to treatments with TeNT, it seems unlikely that cellubrevin is involved in this pathway (Ikonen et al., 1995; Galli et al., 1998). Thus, questions concerning the exact role of cellubrevin in polarized membrane trafficking and its potential connection to adaptor complexes still remain. To better understand the TeNT sensitivity of basolateral sorting and the role of cellubrevin in polarized epithelial cells, we examined MDCK cell lines stably transfected with GFP-cellubrevin (GFP-cb) and TeNT or an enzymatic inactive mutant of TeNT.

Results

Cellubrevin localizes to the basolateral membrane in polarized MDCK cells

Proux-Gillardeaux et al. (2005) established MDCK cells stably transfected with cDNAs encoding cellubrevin tagged with GFP at its N terminus (GFP-cb) and TeNT (+TeNT) or the inactive E234Q mutant of TeNT (+mutant TeNT). Here, we tested the

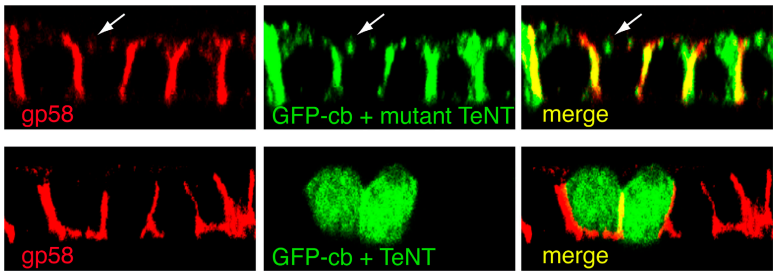

Figure 1. **Cellubrevin colocalizes with gp58 at the basolateral membrane.** Fully polarized MDCK cells stably expressing GFP-cb in conjunction with wild-type (bottom) or mutant (top) TeNT were fixed, permeabilized, and processed for immunofluorescence. Fluorescent staining of gp58 was performed using anti-gp58 antibodies (6.23.3) followed by Alexa 594–labeled secondary antibodies (left, red). Specimens were analyzed by confocal microscopy, and representative X-Z sections are shown. The arrow denotes endosomal structures positive for both gp58 and GFP-cb staining.

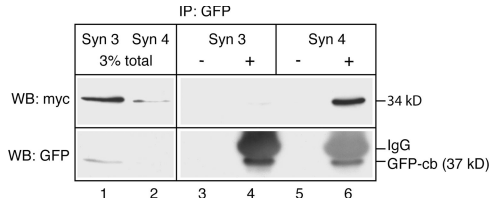

Figure 2. **Syntaxin 4 coprecipitates with GFP-cb.** MDCK cells stably expressing GFP-cb were grown on filter supports, and fully polarized cells were infected with defective adenoviruses expressing myc-tagged versions of syntaxin 3 (Syn 3) or syntaxin 4 (Syn 4). 1 d after infection, cells were lysed and incubated with anti-GFP antibodies. Immunoprecipitates were analyzed by SDS-PAGE and Western blotting using anti-myc (9E10) and anti-GFP antibodies. 3% total indicates 3% of the lysate used for immunoprecipitations.

polarized localization of GFP-cb in filter-grown, fully polarized MDCK cells. As shown in Fig. 1 (top), cellubrevin at least partially colocalized with the marker protein gp58 at the basolateral membrane and in intracellular puncta most likely corresponding to recycling endosomes (Fig. 1, top, arrows). The basolateral localization of GFP-cb may be a result of membrane fusion reactions; therefore, cellubrevin may localize within the basolateral membrane or underneath this domain as part of docked vesicles. It may also be present in early endosomes underlying the basolateral membrane (basolateral early endosomes) after removal from the plasma membrane. To test whether cellubrevin localizes at least in part within the basolateral plasma membrane, we tagged cellubrevin at its luminal, C-terminal end with the myc-epitope (cb-myc). Cb-myc was transiently expressed in polarized MDCK cells. Transfected cells were incubated with anti-myc antibodies before fixation to stain cellubrevin at the membrane. As expected, we detected a fraction of cb-myc at the basolateral surface (Fig. S1, available at http://www.jcb.org/cgi/content/full/jcb.200610047/DC1), confirming the localization observed for GFP-cb. Importantly, we did not detect any surface staining at the apical membrane (Fig. S1).

Coexpression of GFP-cb with TeNT resulted in cleavage of GFP-cb and cytosolic accumulation of GFP (Fig. 1, bottom; Proux-Gillardeaux et al., 2005). Interestingly, stably expressing TeNT in MDCK cells does not lead to a mislocalization of the basolateral marker protein gp58, indicating that overall polarity was not disturbed in this assay (Fig. 1, bottom). Taken together, these data show that cellubrevin localizes in part to the basolateral membrane, where cellubrevin may be involved in fusion events between exocytic vesicles and the basolateral plasma membrane. Moreover, we conclude that the established cell lines coexpressing GFP-cb and TeNT are suitable for analyzing a potential role for cellubrevin in this process.

Cellubrevin forms SNARE complexes with syntaxin 4

To test whether cellubrevin plays a role in fusion events at the basolateral membrane, we sought to coprecipitate cellubrevin with the basolateral t-SNARE syntaxin 4 or the apical t-SNARE syntaxin 3. To this end, we used defective adenoviruses to express myc-tagged versions of syntaxin 4 or 3 in GFP-cb–expressing

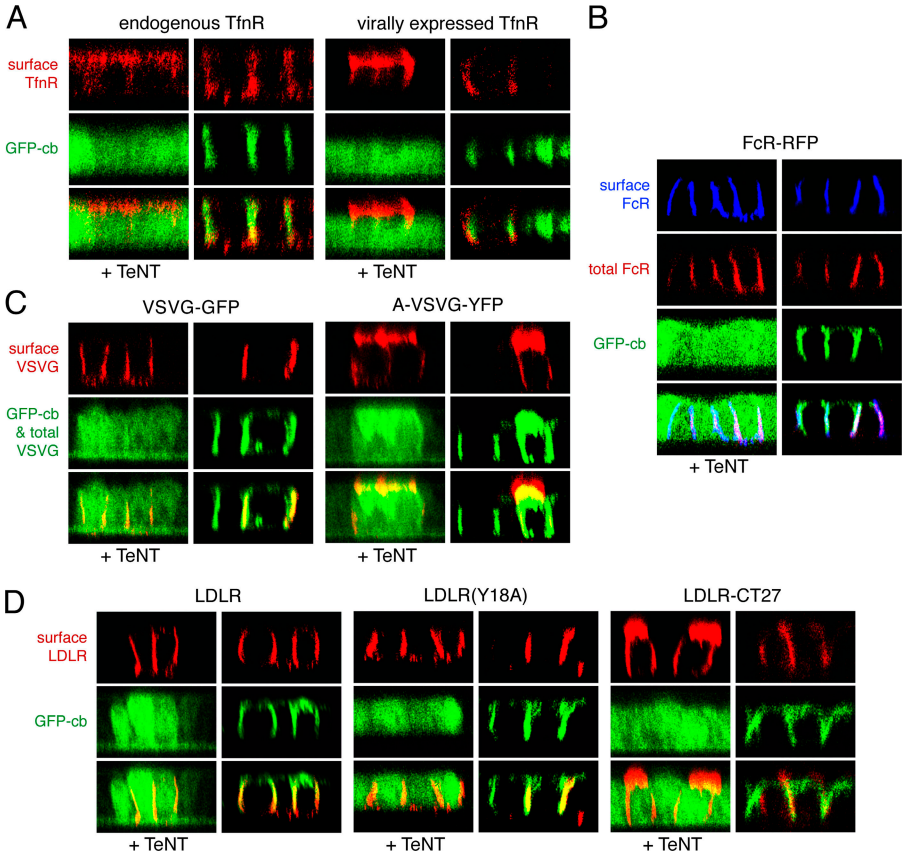

Figure 3. **TeNT inhibits basolateral sorting of TfnR and LDLR-CT27.** MDCK cells expressing GFP-cb and TeNT or mutant TeNT as a control were seeded on polycarbonate filters, allowed to polarize, and infected with defective adenoviruses to drive expression of various surface receptors. (A) TfnR was expressed either endogenously or using an adenovirus vector. Cells were surface stained with anti-TfnR antibodies (OKT9). (B) RFP-tagged FcR (FcR-RFP) expressing cells were surface stained with anti-FcR antibodies (2.4G2). (C) Cells expressing GFP-tagged VSVG or the YFP-tagged A-VSVG were surface stained with anti-VSVG antibodies (TKG). (D) LDLR, LDLR (Y18A), and LDLR-CT27 were visualized by surface staining with anti-LDLR antibodies (C7). After surface staining, cells were fixed, permeabilized, and incubated with secondary antibodies labeled with Alexa 594 (A, C, and D) or Cy5 (B). Images show representative confocal X-Z sections.

MDCK cells. It has previously been shown that myc-tagged syntaxin 3 and 4 localize and function correctly (Kreitzer et al., 2003; Low et al., 2006). As shown in Fig. 2, anti-GFP antibodies efficiently precipitated GFP-cb (lanes 4 and 6). Importantly, although syntaxin 4 was abundantly brought down with cellubrevin (lane 6), only small amounts of syntaxin 3 coprecipitated (lane 4). This shows that cellubrevin preferentially forms SNARE pairs with syntaxin 4. Therefore, we hypothesize that cellubrevin plays a role in some vesicle fusion events at the basolateral plasma membrane in MDCK cells.

TeNT expression results in missorting of TfnR and low-density lipoprotein receptor (LDLR)-CT27

To answer the question of whether cellubrevin is involved in membrane trafficking to the basolateral membrane, we analyzed the sorting phenotypes of various cargos in the presence of TeNT. As shown in Fig. 3 A, endogenous as well as virally expressed TfnR, which have Y-based sorting motifs (Odorizzi and Trowbridge, 1997) and are basolateral in our control cells, showed a nonpolarized distribution in the presence of TeNT. In contrast, FcII-B2 receptors (FcRs), which have an LL-based sorting motif (Matter et al., 1994; Roush et al., 1998), remained localized to the basolateral domain in the presence of TeNT (Fig. 3 B). Next, we tested the surface expression of basolaterally localized VSVG and apical A-VSVG (Toomre et al., 1999). Surprisingly, even though VSVG has a Y-based sorting motif like TfnR (Thomas et al., 1993), this protein remained at the basolateral membrane in the presence of TeNT (Fig. 3 C, left). Importantly, A-VSVG sorting to the apical domain was also not disturbed (Fig. 3 C, right).

Finally, we tested the sorting of LDLR and two of its mutants. LDLR contains two basolateral sorting determinants (Matter et al., 1992). The proximal signal more closely situated toward the transmembrane domain, and surrounding a tyrosine residue at position 18 is an NPXY motif (Bonifacino and Traub, 2003).

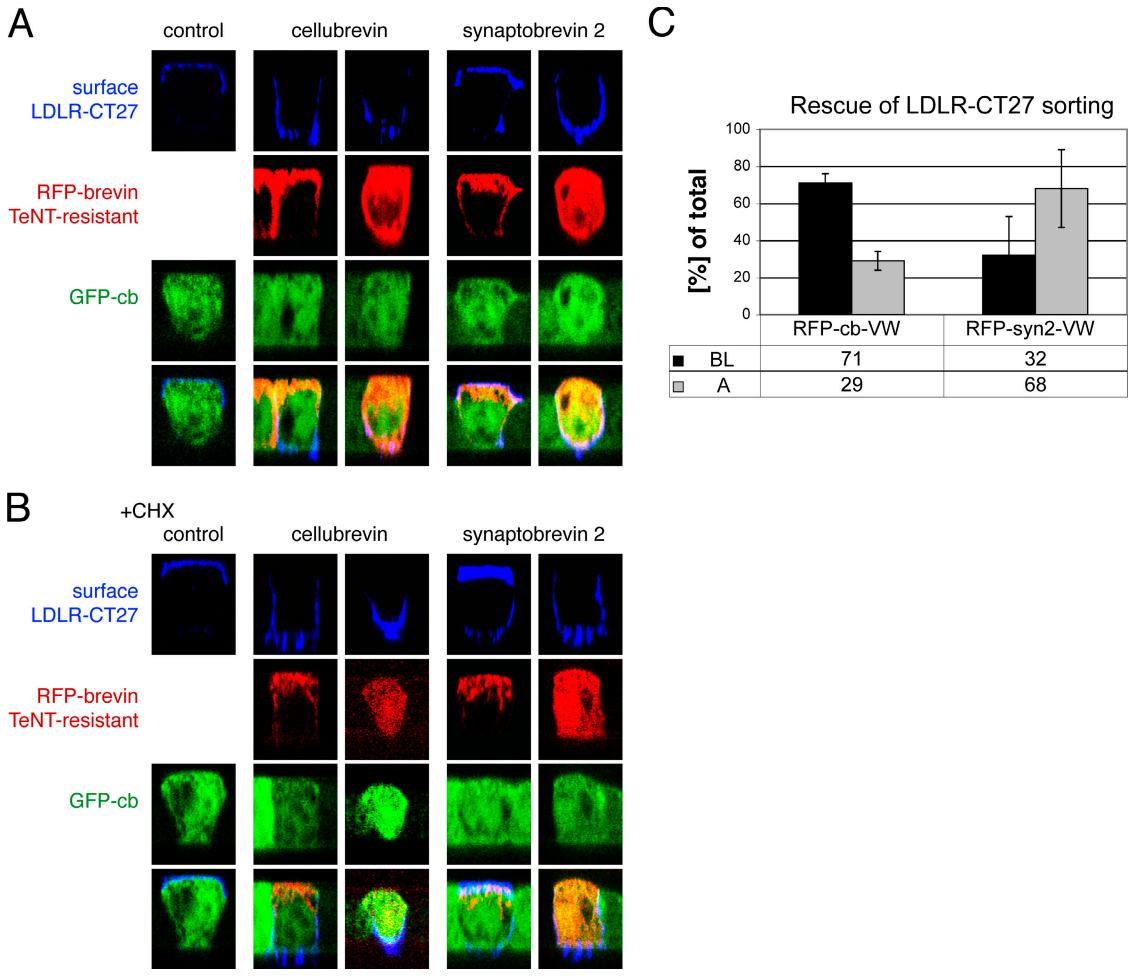

Figure 4. **TeNT-resistant cellubrevin rescues the apical missorting of LDLR-CT27 in the presence of TeNT.** MDCK cells stably expressing GFP-cb and TeNT were seeded on polycarbonate filters and grown for 2 d. Cells were then transiently transfected with cDNAs encoding LDLR-CT27 and TeNT-resistant RFP-cb-VW or RFP-syn2-VW. Transfected cells were incubated for 24 h at 37°C. Cells were either directly stained for surface expression of LDLR-CT27 using anti-LDLR antibodies (C7; A) or treated with 0.1 mg/ml cycloheximide for 2 h at 37°C before surface staining (B). Cells were then fixed, permeabilized, and incubated with Cy5-labeled secondary antibodies. Specimens were analyzed by confocal microscopy, and representative X-Z sections are shown. (C) Cells expressing LDLR-CT27, GFP-cb, and TeNT (judged by cytosolic GFP staining) in conjunction with RFP-cb-VW or RFP-syn2-VW were scored for LDLR-CT27 localization independent of RFP-cb-VW or RFP-syn2-VW expression levels. Data represent mean values from four independent experiments, and error bars indicate SEM.

By contrast, the distal targeting determinant is considered a non-canonical Y-based motif (Fölsch et al., 1999). The first mutant receptor analyzed was LDLR(Y18A), in which the critical tyrosine 18 was mutated to an alanine. The second mutant construct was truncated at position 27, right after the proximal targeting determinant (LDLR-CT27). We found that sorting of LDLR and LDLR(Y18A) is insensitive to TeNT (Fig. 3 D, left). In contrast, LDLR-CT27 was missorted in the presence of TeNT (Fig. 3 D, right). Therefore, only basolateral targeting mediated by LDLR's proximal sorting determinant is sensitive to TeNT expression. In summary, we found that two basolateral receptors, TfnR and LDLR-CT27, are missorted to the apical domain when TeNT is present.

TeNT-resistant cellubrevin rescues missorting of LDLR-CT27 induced by TeNT

Next, we performed rescue experiments to confirm that cleavage of cellubrevin is the reason for the observed TeNT sensitivity of basolateral sorting. There are only three known v-SNAREs that are substrates for TeNT. However, although cellubrevin and synaptobrevin 2 are cleaved very efficiently, cleavage of synaptobrevin 1 is less efficient (Schiavo et al., 1992; Yamasaki et al., 1994). Moreover, although cellubrevin is ubiquitously expressed, synaptobrevin 1 and 2 could not be detected in MDCK cells by Western blotting (Proux-Gillardeaux et al., 2005). Therefore, to analyze rescue, we added an N-terminal RFP tag to TeNT-resistant mutants of human cellubrevin (RFP-cb-VW) and, for control purposes, human synaptobrevin 2 (RFP-syn2-VW) by mutating Q63/F64 or Q76/F77 to VW (Regazzi et al., 1996), respectively. These constructs, together with LDLR-CT27, were transiently expressed in MDCK cells stably expressing TeNT and GFP-cb. Cells were processed for surface staining of LDLR-CT27 with or without inhibiting protein synthesis with cycloheximide for 2 h before fixation. As shown in Fig. 4, RFP-cb-VW rescued the basolateral sorting of LDLR-CT27 independently of expression levels in ∼70% of all analyzed cells (cells showing lower levels of RFP-cb-VW expression are shown in the left panels). Furthermore, this rescue was independent of ongoing protein synthesis (Fig. 4 B). In contrast, RFP-syn2-VW rescued only if highly overexpressed (Fig. 4, A and B, RFP-syn2-VW, compare right and left panels). Again, the same result was obtained after adding cycloheximide. Overall, RFP-syn2-VW rescued LDLR-27 sorting in ∼30% of all cells analyzed, counting cells independent of their expression levels (Fig. 4 C).

Next, we transiently expressed RFP-cb-VW or RPF-syn2-VW in the cell line stably expressing GFP-cb and found that RFP-cb-VW colocalized with GFP-cb in endosomes and at the plasma membrane, whereas RFP-syn2-VW only partially co localized with GFP-cb in endosomes (Fig. S2, available at http://www.jcb.org/cgi/content/full/jcb.200610047/DC1). In addition, we could barely detect RFP-syn2-VW at the plasma membrane (Fig. S2), indicating that even if synaptobrevin 2 were expressed in MDCK cells, it is not likely to be involved in fusion events at the basolateral plasma membrane. In summary, from these rescue experiments, we conclude that cellubrevin is indeed the v-SNARE needed for basolateral sorting.

Biosynthetic delivery of LDLR-CT27 is TeNT sensitive

LDLR-CT27 is a receptor that is internalized rapidly from the plasma membrane (Matter et al., 1992). Therefore, by analyzing LDLR-CT27 missorting at steady state, we can so far make the conclusion that LDLR-CT27 is dependent on cellubrevin function during endocytic recycling. To address the question of whether there might already be a TeNT-sensitive step in LDLR-CT27 sorting during biosynthetic delivery, we performed radioactive pulse-chase experiments coupled to vectorial surface biotinylation with MDCK cells stably expressing GFP-cb and TeNT or its enzymatic mutant and virally expressing LDLR-CT27. Surprisingly, after a 1-h chase, newly synthesized LDLR-CT27 arrived directly at the apical surface (Fig. 5 A). The same was true for earlier time points (30 min), when newly synthesized LDLR-CT27 starts to appear at the plasma membrane (unpublished data). The overall apical missorting measured by this pulse-chase experiment is only ∼50% and seems weaker than the sorting phenotypes observed by immunofluorescence. However, our cell lines were not clonal, as judged by the fact that not all cells in the population expressed GFP-cb and TeNT (compare Figs. 1, 3, and 4 for appearance of cells without GFP staining). As a result, the coinfection rate of GFP-cb– and TeNT-expressing cells with LDLR-CT27 virus was only ∼50%. As expected, LDLR-CT27 was directly sorted to the basolateral membrane in our control cell lines expressing mutant TeNT (Fig. 5 B). Therefore, it

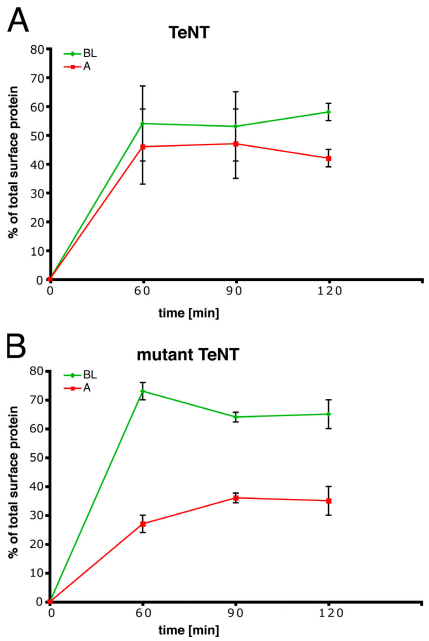

Figure 5. **TeNT leads to missorting of LDLR-CT27 during biosynthetic delivery.** MDCK cells expressing GFP-cb and TeNT (A) or mutant TeNT (B) were seeded on polycarbonate filters, and fully polarized cells were infected with defective adenoviruses encoding LDLR-CT27. 24 h after infection, cells were pulse-labeled with [^{35}S]Met/Cys, followed by a chase, surface biotinylation, and immunoprecipitations as described in Materials and methods. Samples were run on SDS gels and exposed to Phosphorimager plates. Shown are the graphical representations of the quantification of the surface expression of LDLR-CT27. Experiments were repeated three times, and error bars indicate SEM.

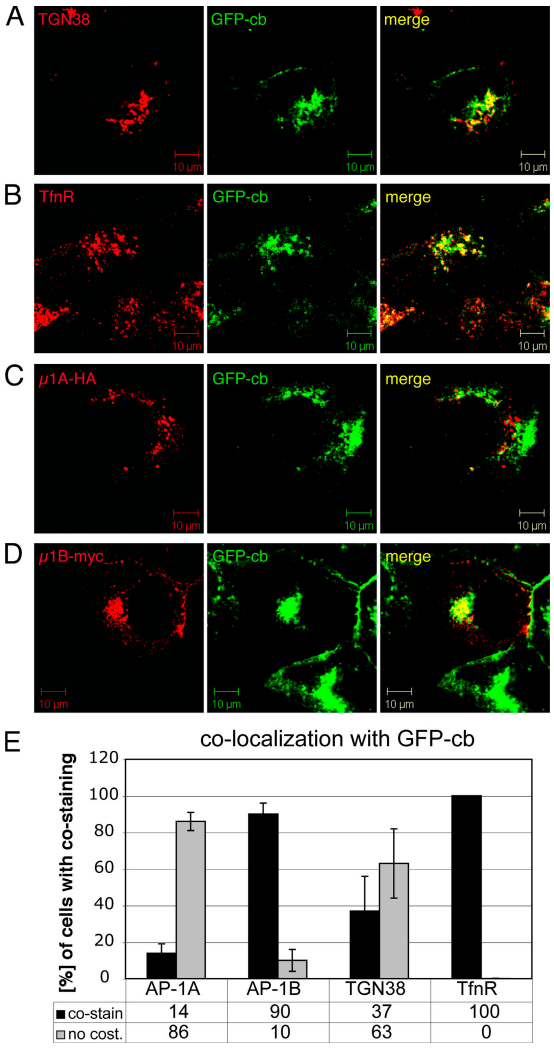

Figure 6. **Cellubrevin localizes to AP-1B–positive recycling endosomes.** (A and B) MDCK cells expressing GFP-cb were grown on coverslips for 2 d and then transfected with cDNA expressing TGN38 or TfnR. After a 24-h incubation, TGN38-expressing cells were fixed directly, and coverslips with cells expressing TfnR were incubated for 2 h at 20°C before fixation. Fixed cells were immunolabeled for TGN38 (A, red) or TfnR (H68.4 antibodies; B, red). (C and D) MDCK cells expressing GFP-cb were grown on coverslips for 2 d and then infected with defective adenoviruses expressing μ1A-HA or μ1B-myc. After a 36-h incubation, cells were fixed, permeabilized, and immunolabeled for HA (C, red) or myc (D, red). Specimens were analyzed by confocal microscopy, and representative images are shown. Bars, 10 μm. (E) Cells with similar expression levels of GFP-cb and various marker proteins were scored for colocalization of both markers. Data represent mean values from at least three independent experiments. Error bars indicate SEM.

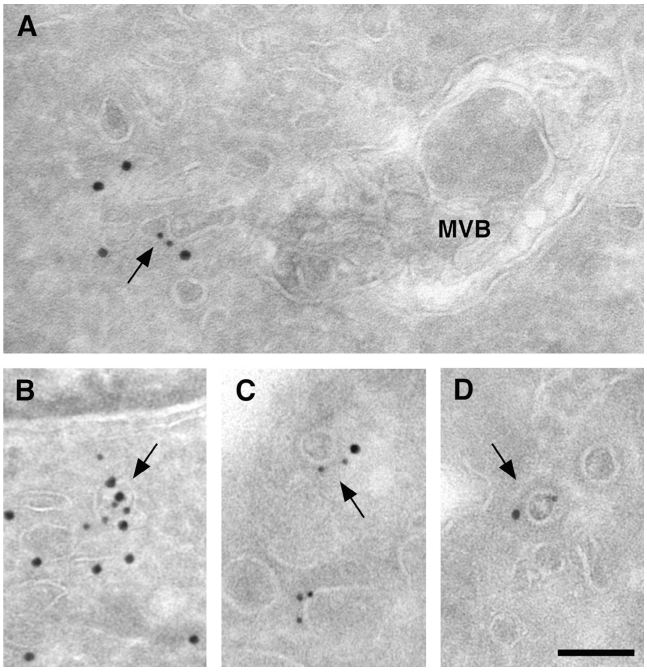

Figure 7. **Cellubrevin localizes to AP-1B–positive endosomes and clathrin-coated vesicles.** MDCK cells stably expressing GFP-cb were grown to confluency in T25 flasks and infected with defective adenoviruses encoding μ1B-myc. 36 h after infection, cells were fixed and prepared for immuno-EM as described in Materials and methods. Specimens were labeled for myc (10 nm gold) and GFP (15 nm gold) staining. Arrows denote structures showing colocalization of GFP-cb and μ1B-myc. MVB, multivesicular body. Bar, 100 nm.

seems that the sorting of LDLR-CT27 is already sensitive to TeNT during biosynthetic delivery in addition to missorting during recycling.

Cellubrevin colocalizes with TfnR and AP-1B

To further analyze which basolateral sorting pathways might depend on cellubrevin, we analyzed cellubrevin's subcellular localization by indirect immunofluorescence. We found that in addition to the plasma membrane, GFP-cb localized to a perinuclear region distinct from the Golgi complex, as demonstrated by costaining with the cis-Golgi marker GM130 (unpublished data) and on endosomal populations throughout the cells. Furthermore, cellubrevin showed in ∼60% of all cells analyzed staining patterns distinct from TGN38, a marker for AP-1A–positive TGN subdomains (Fölsch et al., 2003; Fig. 6, A and E). In contrast, in virtually all cells analyzed, cellubrevin showed colocalization with TfnR accumulated in recycling endosomes by incubating the cells for 2 h at 20°C before fixation (Fig. 6, B and E). Moreover, cellubrevin partially colocalized with γ-adaptin, one of the large subunits of AP-1A and AP-1B (unpublished data). To directly compare cellubrevin's localization relative to AP-1A or AP-1B, we used defective adenoviruses to express HA-tagged μ1A or myc-tagged μ1B (Fölsch et al., 2003). Again, there was only limited colocalization between GFP-cb and AP-1A–HA (only in ∼15% of the cells analyzed), but we observed colocalization between GFP-cb and AP-1B–myc in 90% of the cells expressing both markers (Fig. 6, C, D, and E). Finally, as additional controls, we analyzed cellubrevin tagged at the N or C terminus with the myc epitope transiently expressed in MDCK cells (myc-cb and cb-myc). The myc-tagged cellubrevin proteins confirmed our analysis with GFP-cb. Myc-cb and cb-myc both colocalized with TfnR and showed essentially the same endosomal and plasma membrane staining pattern as GFP-cb (unpublished data).

In addition to immunofluorescence analysis, we investigated the colocalization of cellubrevin and AP-1B ultrastructurally by immuno-EM on specimens stably expressing GFP-cb and transiently expressing μ1B-myc. As shown in Fig. 7, we detected

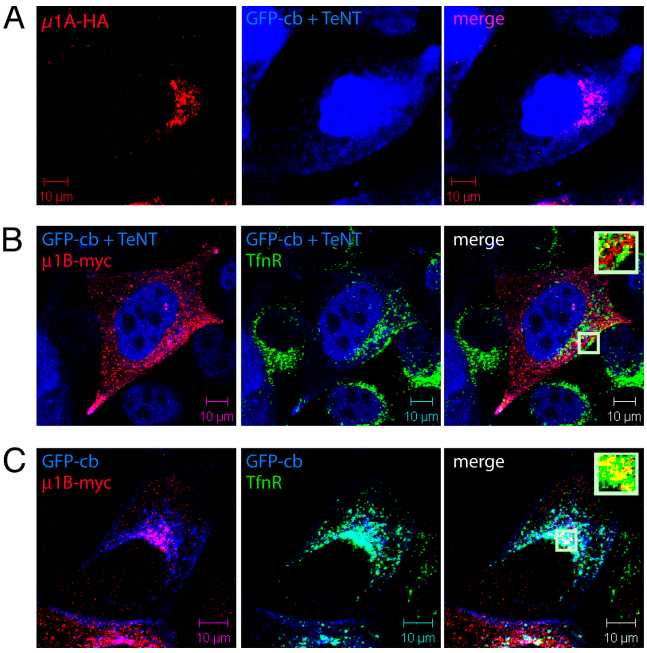

Figure 8. **AP-1B localization is dispersed in TeNT-expressing cells.** MDCK cells stably expressing GFP-cb (false color blue) and TeNT or mutant TeNT were grown on coverslips for 2 d and infected with defective adenoviruses expressing μ1A-HA or μ1B-myc. 36 h after infection, cells were fixed and processed for immunofluorescence staining with antibodies against HA (16B12 → goat anti-mouse Alexa 594; A) or myc (A-14 → goat anti-rabbit Alexa 594) and TfnR (H68.4 → goat anti-mouse Cy5; false color green; B and C). Specimens were analyzed by confocal microscopy, and representative images are shown. The boxed areas are shown enlarged as insets in the top right corner of the merged image showing only red (μ1B-myc) and green (TfnR) staining. Bars, 10 μm.

colocalization of cellubrevin (15 nm gold) and AP-1B–myc (10 nm gold) in endosomes (Fig. 7, A and B, arrows) and in clathrin-coated vesicles (Fig. 7, C and D, arrows). As expected from the immunofluorescence data, we also found cellubrevin in endosomal populations negative for AP-1B labeling, which perhaps represent early endosomes. In summary, we conclude that cellubrevin colocalizes with AP-1B in recycling endosomes and clathrin-coated vesicles.

TeNT expression disrupts the perinuclear localization of AP-1B

Given that TfnR, cellubrevin, and AP-1B all localize to recycling endosomes, we asked whether cleavage of cellubrevin by TeNT interferes with the colocalization of TfnR and AP-1B in this compartment. Thus, we virally expressed μ1A-HA or μ1B-myc in MDCK cells stably expressing GFP-cb (false color blue) and TeNT or mutant TeNT. As shown in Fig. 8 A, TeNT expression had no effect on the perinuclear localization of AP-1A–HA in ∼90% of the cells analyzed (data counts not depicted). However, AP-1B–myc staining was scattered throughout the cell in >95% of the cells analyzed (Fig. 8 B; data counts not depicted). Moreover, costaining for TfnR (false color green) revealed that TfnR staining was also more dispersed in cells stably expressing TeNT as compared with the control cells without TeNT. Most important, although in control cells AP-1B–myc and TfnR colocalized at recycling endosomes together with GFP-cb (Fig. 8 C; note extensive yellow staining in magnified inset), AP-1B–myc and TfnR no longer colocalized after cleavage of cellubrevin (Fig. 8 B; note distinct red and green staining in magnified inset). Therefore, in addition to cellubrevin's role in membrane fusion at the basolateral plasma membrane, as evidenced by observed SNARE pairing between cellubrevin and syntaxin 4 (Fig. 2), cellubrevin may be required for the homeostasis of recycling endosomes. Furthermore, the selective disruption of AP-1B staining suggests that cellubrevin plays a role in AP-1B–mediated basolateral targeting.

TfnR and LDLR-CT27 are AP-1B–dependent basolateral cargos

Because AP-1B's localization at recycling endosomes depends on functional cellubrevin, we asked which cargos analyzed in this study are AP-1B dependent and whether there is a correlation between AP-1B dependency and TeNT sensitivity in basolateral sorting. In the past, we designated basolateral transmembrane proteins as AP-1B dependent for sorting based on their behavior in the μ1B-negative porcine kidney epithelial cell line LLC-PK1 (Fölsch et al., 1999). In this cell line, receptors with Y-based sorting motifs, such as TfnR, LDLR, and VSVG, were missorted to the apical domain, and this sorting phenotype was reversed by exogenously expressing μ1B in LLC-PK1 cells (LLC-PK1::μ1B; Fölsch et al., 1999, 2003; Table I). In contrast, receptors with LL-based signals, such as FcR, remained located to the basolateral domain independent of μ1B expression (Roush et al., 1998). However, the sorting data available in LLC-PK1 cells were not complete. Therefore, we investigated sorting behaviors of additional cargos in LLC-PK1::μ1A, LLC-PK1::μ1B, or LLC-PK1 cells expressing a mutated μ1B (LLC-PK1::$\mu1B^{mut}$). $\mu1B^{mut}$ has four mutations (F172A, D174A, W408A, and R410A), which abolish μ1B's binding to sorting peptides (Sugimoto et al., 2002).

First, we analyzed LDLR and its mutants LDLR-CT27 (proximal signal intact) and LDLR(Y18A) (distal signal intact). As shown in Table I and Fig. S3 (available at http://www.jcb.org/cgi/content/full/jcb.200610047/DC1), we found that LDLR and LDLR-CT27, which are basolateral in MDCK cells, are apical in LLC-PK1::μ1A cells. In both cases, basolateral sorting was restored in LLC-PK1::μ1B cells (Table I; Fölsch et al., 1999). However, only LDLR-CT27 showed a missorting phenotype in LLC-PK1::$\mu1B^{mut}$ cells. The different sorting behaviors of LDLR and LDLR-CT27 might be explained if the distal signal is AP-1B independent. Indeed, LDLR(Y18A) was localized to the basolateral membrane independent of μ1B expression (Table I; Gan et al., 2002). Next, we analyzed TfnR and VSVG. Both cargos are apical in LLC-PK1::μ1A cells and basolateral in LLC-PK1 cells expressing μ1B. Surprisingly, basolateral sorting of TfnR and VSVG was also restored in LLC-PK1 cells expressing $\mu1B^{mut}$ (Table I; Fölsch et al., 1999, 2003; Sugimoto et al., 2002). The reason for this lack of missorting could be either that $\mu1B^{mut}$ still binds to the respective sorting signals or that TfnR and VSVG interact with putative (AP-1B) coadaptors instead. As expected, FcR and A-VSVG were sorted to the basolateral or apical domain, respectively, in all cell lines tested (Table I; Roush et al., 1998; Fölsch et al., 2003).

Table I. **Sorting phenotypes in different epithelial cell lines**

	LLC-PK1			MDCK
	μ1A	**μ1B**	**μ1B^{mut}**	**TeNT**
LDLR	A[a,b]	BL[a,b]	BL[b]	BL[e]
LDLR(Y18A)	BL[e]	BL[e]	BL[e]	BL[e]
LDLR-CT27	A[e]	BL[e]	A[e]	A[e]
TfnR	A[a,b]	BL[a,b]	BL[b]	A[e]
VSVG	A[c]	BL[c]	BL[e]	BL[e]
A-VSVG	A[e]	A[c]	A[e]	A[e]
FcR	BL[d,e]	BL[e]	BL[e]	BL[e]

Sorting phenotypes of cargo receptors in individual cell lines were obtained as described in Materials and methods. A, apical localization; BL, basolateral localization.
[a]Fölsch et al., 1999.
[b]Sugimoto et al., 2002.
[c]Fölsch et al., 2003.
[d]Roush et al., 1998.
[e]This study. Representative images of confocal X-Z sections are shown in Fig. S3 (available at http://www.jcb.org/cgi/content/full/jcb.200610047/DC1).

To gain a better understanding of which alternative adaptor complexes might be involved in basolateral sorting of LDLR(Y18A), TfnR, and VSVG, we tested by yeast two-hybrid assay the interactions of individual sorting signals with various μ-chains (μ1A, μ1B, μ1B^{mut}, μ2, μ3A, or μ4). To this end, we analyzed the proximal and distal sorting determinants of LDLR and TfnR, as well as the sorting signal of VSVG. As a positive control, we also analyzed the sorting signal of TGN38 (Table II and Fig. S4, available at http://www.jcb.org/cgi/content/full/jcb.200610047/DC1). For LDLR, we found that the distal targeting signal GYSY (present in LDLR[Y18A]) interacted with μ2, μ3A, and μ4, suggesting that LDLR(Y18A) may use AP-3 or AP-4 to exit the TGN. In contrast, the proximal targeting signal of LDLR, NPXY (present in LDLR-CT27), does not interact with any of the μ-chains. However, it should be noted that although the NPXY signal is a well-established endocytic signal, AP-2 does not bind directly to NPXY. In the case of LDLR, this interaction is bridged by the coadaptors ARH/Dab2/numb (Traub, 2003). Perhaps similar coadaptors are involved in LDLR sorting from recycling endosomes.

TfnR also has two sorting determinants. One is the proximal, endocytic signal YTRF, and the other is the distal signal GNDS, thought to be involved in correct recycling of TfnR (Odorizzi and Trowbridge, 1997). We found no interactions between the GNDS signal and any μ-chains. In contrast, we found interactions for the YTRF motif with all μ-chains tested. The strongest interactions were observed between YTRF and μ2/μ4, suggesting that TfnR may use AP-4 to exit the TGN during biosynthetic delivery. As expected, we detected no interactions with the mutant μ1B^{mut} (Fig. S4 B). The situation was similar for TGN38, whose sorting signal (Bos et al., 1993) also interacted with all tested μ-chains (strongest with μ3A and μ4). Finally, the YTDI signal of VSVG (Thomas et al., 1993) interacted with μ1B and, to a weaker extent, with μ4. Interestingly, the interaction between YTDI and μ1B was not disrupted when tested against μ1B^{mut} (Fig. S4 B), which may explain why VSVG is not missorted to the apical domain in LLC-PK1::μ1B^{mut} cells.

In summary, we observed that most of the basolateral sorting signals interact with multiple adaptor complex μ-chains, including μ1B. The interaction with alternative adaptor complexes, most notably AP-4, may be involved in basolateral targeting during biosynthetic delivery, whereas AP-1B may be used during recycling (TfnR, LDLR-CT27, and VSVG) and biosynthetic delivery (LDLR-CT27 and VSVG). Interestingly, with the exception of VSVG, AP-1B dependency seems to correlate well with sensitivity to TeNT.

Discussion

SNARE proteins are fundamentally important for all known intracellular fusion events between transport vesicles and target membranes. For example, apical targeting depends on the correct sorting of syntaxin 3 to the apical domain, and its missorting to the basolateral domain results in loss of cellular polarity (Kreitzer et al., 2003; ter Beest et al., 2005; Sharma et al., 2006). Furthermore, at the apical membrane syntaxin 3 forms SNARE pairs with the v-SNARE, TI-VAMP, and SNAP-23 (Galli et al., 1998). The SNARE pairs involved in basolateral sorting, however, remained elusive. Using TeNT-expressing MDCK cells, we have now provided evidence that at least a subset of basolateral vesicles uses cellubrevin for basolateral sorting. Moreover, we were able to coprecipitate cellubrevin with the basolaterally localized syntaxin 4, indicating that syntaxin 4 and cellubrevin form SNARE pairs during exocytosis at the basolateral membrane.

Besides the basolateral membrane, we found cellubrevin localizing to different endosomal populations, including TfnR and AP-1B–positive recycling endosomes. These data fit very well with previous studies demonstrating a role for cellubrevin in TfnR recycling from recycling endosomes in fibroblasts (Galli et al., 1994; Daro et al., 1996). In addition, by immuno-EM, we found cellubrevin colocalizing with AP-1B in endosomes and clathrin-coated vesicles. It has previously been shown that some v-SNAREs directly interact with APs. For example, the TGN-localized VAMP 4 has an LL-based motif needed for interaction with AP-1 (Peden et al., 2001). Similarly, TI-VAMP interacts with δ-adaptin/AP-3 through its aminoterminal longin domain (Martinez-Arca et al., 2003). However, we found no

Table II. **Yeast two-hybrid interactions of μ-chains with sorting signals**

Protein	Signal	Growth on TDO	Growth on TDO + 1 mM 3-AT	Growth on QDO
LDLR (proximal)	NPVYQKT	—	—	—
LDLR (distal)	QDGYSYPSR	μ2, μ3A, and μ4	—	—
TfnR (proximal)	PLSYTRF	μ1A, μ1B, μ2, μ3A, and μ4	μ2 and μ4	μ4
TfnR (distal)	VDGNDSHV	—	—	—
TGN38	ASDYQRL	μ1A, μ1B, μ2, μ3A, and μ4	μ2, μ3A, and μ4	μ3A and μ4
VSVG	RQIYTDI	μ1B, $\mu1B^{mut}$, and μ4	μ1B and $\mu1B^{mut}$	—

Data were obtained as described in Materials and methods, and images of yeast plates showing growth of cotransformants on selective media are shown in Fig. S4 (available at http://www.jcb.org/cgi/content/full/jcb.200610047/DC1). TDO, triple dropout; QDO, quadruple dropout. 3-AT, 3-amino-1,2,4-triazole.

evidence that AP-1B directly recognizes cellubrevin and, at least by yeast two-hybrid assay, cellubrevin failed to interact with μ1B (unpublished data). Therefore, we propose that cellubrevin is incorporated into AP-1B vesicles through interactions with putative coadaptors. For instance, in mammalian cells, EpsinR helps incorporating Vti1b into AP-1A vesicles at the TGN (Chidambaram et al., 2004; Hirst et al., 2004). Likewise, in yeast cells, the EpsinR homologue Ent3p interacts specifically with Vti1p (Chidambaram et al., 2004). Future experiments will be aimed at identifying putative coadaptors for AP-1B coats that might help incorporating cellubrevin into AP-1B vesicles.

Interestingly, the cleavage of cellubrevin by TeNT results not only in a more scattered endosomal staining of TfnR but also in a loss of perinuclear AP-1B staining. Because the colocalization of TfnR and AP-1B was lost also, these data suggest a role for cellubrevin in maintaining functional recycling endosomes. It seems that without cellubrevin, cargo such as TfnR can no longer enter this compartment. Alternatively, fusion-incompetent AP-1B vesicles may titer out components needed to generate new vesicles, also leading to a disruption of recycling endosomes (indicated in Fig. 9 B as isolated entities as opposed to the normal tubular network [Fig. 9 A]). Without functional (AP-1B–positive) recycling endosomes, however, cargo that is normally sorted into AP-1B vesicles at recycling endosomes for basolateral delivery will be missorted to the apical membrane if no alternative pathways can be used instead.

It has been noted that the rate of basolateral delivery of VSVG, but not the apical delivery of influenza HA protein, is sensitive to treatment with TeNT (Ikonen et al., 1995). In this study, we show that apical cargos (A-VSVG) and AP-1B–independent basolateral cargos (LDLR[Y18A] and FcR) are sorted correctly to the apical or basolateral domain, respectively, independent of functional cellubrevin. Although we still do not know which adaptor complex sorts FcR to the basolateral membrane, based on yeast two-hybrid interactions, we propose that LDLR(Y18A) is sorted by AP-4, as has been suggested previously for wild-type LDLR (Simmen et al., 2002). In contrast, we observed apical missorting of the AP-1B–dependent cargos TfnR and LDLR-CT27. Surprisingly, however, VSVG, the protein perhaps most often used in the literature as "AP-1B–dependent" cargo, was not missorted. These data are summarized in Fig. 9. Although Fig. 9 A shows the situation without TeNT, Fig. 9 B shows the scenario with TeNT. For simplicity, we are omitting sorting into lysosomes and retrieval pathways.

We found that LDLR-CT27 is missorted during recycling at steady state (Figs. 3 and 4) and directly during biosynthetic delivery (Fig. 5). The latter finding suggests that LDLR-CT27 normally traffics to the basolateral surface via recycling endosomes and that no alternative pathways exist. Indeed, we found no interaction between LDLR-CT27 and any adaptor complex μ-chains, and this receptor was entirely dependent on AP-1B for basolateral sorting (Tables I and II). In agreement with this, we previously demonstrated that LDLR specifically cross-linked to AP-1B (Fölsch et al., 2001). In addition, LDLR-CT27's AP-1B dependence was recently underlined by its apical missorting in MDCK cells, in which μ1B was knocked down by siRNA (Maday, S., and I. Mellman, personal communication). Like LDLR-CT27, TfnR is missorted during recycling. However, unlike LDLR-CT27, TfnR interacted well with alternative adaptor complex μ-chains (Table II). We propose that during biosynthetic delivery, TfnR is sorted via AP-4 directly from the TGN to the basolateral membrane. In agreement with this, a small fraction of TfnR was missorted in MDCK cells incubated with μ4 anti-sense RNA (Simmen et al., 2002). Furthermore, Gravotta et al. (2007) showed that knock down of μ1B in MDCK cells by siRNA resulted in missorting of TfnR during recycling, but not during biosynthetic delivery, also indicating that newly synthesized TfnR may be sorted directly from the TGN to the basolateral membrane.

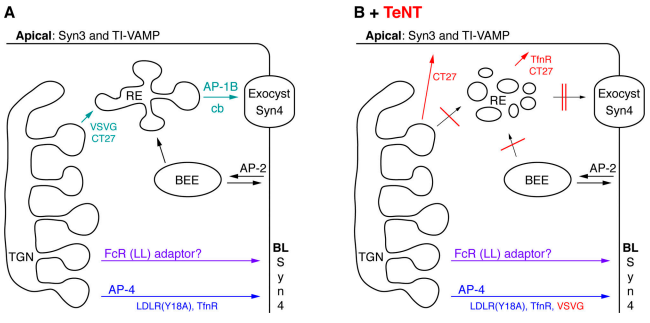

Figure 9. **Model of cellubrevin function in polarized epithelial cells.** Depicted in this model are the main sorting pathways relevant for the fate of the analyzed cargo. (A) Situation without TeNT; (B) alteration of sorting pathways after cleavage of cellubrevin by TeNT. Note that retrieval pathways to the TGN as well as lysosomal sorting have been omitted from the model for reasons of simplicity. The red lines in B denote pathways that are blocked (two lines) and most likely blocked (one line) when cellubrevin is cleaved. CT27, LDLR-CT27; RE, recycling endosomes; BEE, basolateral early endosome; Syn, syntaxin.

We previously found that VSVG sorting to the basolateral membrane was AP-1B dependent (Fölsch et al., 2003), and this cargo was used in studies to link small GTPases to the AP-1B pathway (Ang et al., 2003). Furthermore, we showed that VSVG moves through recycling endosomes during biosynthetic delivery in semipolarized MDCK cells, indicating an involvement of AP-1B during biosynthetic delivery (Ang et al., 2004). Therefore, we expected to see a missorting phenotype for VSVG in TeNT-expressing MDCK cells. It should be noted however, that tailless VSVG or VSVG with a mutated Y-based motif showed only weak apical missorting (33 and 37%, respectively; Thomas et al., 1993). Furthermore, in MDCK cells incubated with μ1B siRNA, biosynthetic delivery of VSVG to the basolateral membrane still occurred at ∼60% (Gravotta et al., 2007). Therefore, VSVG may use alternative sorting pathways in the absence of AP-1B or functional sorting signals. The use of alternative adaptor complexes by VSVG may be more pronounced in cells with dysfunctional recycling endosomes because of the expression of TeNT. Indeed, when recycling endosomes were inactivated enzymatically, the majority of VSVG was retained within the cells, but a small fraction was delivered to the basolateral membrane (Ang et al., 2004). VSVG was shown to interact with δ-adaptin/AP-3 (Nishimura et al., 2002); however, AP-3's main function is to facilitate lysosomal sorting and not plasma membrane delivery. Here, we show by yeast two-hybrid analysis that VSVG interacts with μ4 (Table II). Thus, we propose that VSVG may use AP-4 as an alternative adaptor complex to reach the basolateral membrane. The interplay and possible competition of the different adaptors binding VSVG (AP-1B, AP-3, and AP-4) should now be sorted.

In conclusion, we found that, in general, cellubrevin is needed for basolateral sorting of AP-1B–dependent cargo. In addition, this v-SNARE is required for maintaining functional (AP-1B–positive) recycling endosomes. Collectively, these data strongly suggest a functional connection between cellubrevin and AP-1B in membrane trafficking to the basolateral domain.

Materials and methods

Cloning RFP-tagged TeNT-resistant cellubrevin and synaptobrevin 2 and myc-tagged cellubrevin

RFP-tagged versions of TeNT-resistant cellubrevin and synaptobrevin 2 were cloned by PCR-based site-directed mutagenesis using human cellubrevin cDNA (Proux-Gillardeaux et al., 2005) and human synaptobrevin 2 cDNA (OriGene Technologies) as templates using the following C-terminal 5′-CTTGGCTGCGCTCGTTTCCCATACAGAAGCGCCTGCCTGCAG-3′ and N-terminal primers 5′-CTGCAGGCAGGCGCTTCTGTATGGGAAACGAGCGCAGCCAAG-3′ to generate cellubrevin(Q63V/F64W) and C-terminal 5′-GCTTGGCTGCGCTTGTTTCCCACACGGAGGCCCCCGCCTGGAG-3′ and N-terminal primers 5′-CTCCAGGCGGGGGCCTCCGTGTGGGAAACAAGCGCAGCCAAGC-3′ to generate synaptobrevin 2(Q76V/F77W). Subsequently, mutated cellubrevin or synaptobrevin 2 was amplified by PCR and cloned into pRKV-RFP as BamHI–HindIII fragments. PRKV-RFP was generated by amplifying RFP as EcoRI–BamHI PCR fragments using FcR-RFP as template. PCR products were verified by sequencing, and no errors were found.

N- and C-terminal myc tags were introduced into cellubrevin by PCR using human cellubrevin cDNA as template as above and exchanging the N- or C-terminal primers with 5′-GCGCGGATCCGAACAAAAGCTGATTTCTGAAGAAGACTTGATGTCTACAGGTCCAACTGCTGCC-3′ or 5′-GCGCAAGCTTTCACAAGTCTTCTTCAGAAATCAGCTTTTGTTCTGAAGAGACAACCCACACGATGATG-3′, respectively.

Cloning sorting peptides for yeast two-hybrid analysis

Sorting peptides as indicated in Table II were translated into DNA sequences and amplified by PCR as overhangs introducing an EcoRI site at the N terminus for cloning into the multiple cloning site of pAS2-1. As C-terminal primer, we used a sequence priming ∼1 kbp downstream of the multiple cloning site: 5′-CCTGTTACTAGTGGCTGCTGCCAG–3′. The PCR products were cloned as EcoRI–SpeI fragments into pAS2-1. As a result, the sorting peptides were fused in frame with the Gal4 binding domain. The constructs were verified by sequencing, and no errors were found. The different μ-chains cloned into pACT-2 as fusions with the Gal4 activating domain, were a gift from J. Bonifacino (National Institutes of Health, Bethesda, MD). $\mu1B^{mut}$ was amplified using PCR from cell extracts of LLC-PK1::$\mu1B^{mut}$ cells and cloned into pACT2.

Plasmids were cotransformed into the yeast AH109, and positive transformants were selected for growth on plates minus Trp and Leu. Subsequently, positive interactions between bait and prey constructs were tested on selective media lacking, in addition, His or His and Ade. If indicated, 1 mM 3-amino-1,2,4-triazole was added.

Recombinant adenoviruses, constructs, and antibodies

Defective adenoviruses encoding LDLR, TfnR, VSVG-ts045-GFP, or A-VSVG-ts045-YFP were as described previously (Fölsch et al., 1999, 2003). Defective adenoviruses encoding LDLR(Y18A), LDLR-CT27, or FcR-RFP were prepared by homologous recombination as described previously (Fölsch et al., 1999). FcR-RFP cDNA in pShuttle was a gift from I. Mellman (Yale University, New Haven, CT), and myc-tagged syntaxin 3 or 4 in pShuttle was a gift from T. Weimbs (University of California, Santa Barbara, Santa Barbara, CA).

Mouse monoclonal antibodies were purchased as follows: anti-HA (16B12) from BabCo, anti-GM130 (610822) and anti-TGN38 (T69020) from BD Biosciences, anti-γ (100:3) from Sigma-Aldrich, and anti-TfnR (OKT9) from eBioscience. Rabbit polyclonal anti-GFP antibodies were purchased from Abcam, and rabbit anti-myc antibodies (A-14) were purchased from Santa Cruz Biotechnology, Inc. Hybridomas producing anti-hTfnR (H68.4), anti-myc (9E10), anti-LDLR (C7), or anti-FcR (2.4G2) antibodies were purchased from American Type Culture Collection. Hybridomas producing antibodies directed against gp58 (6.23.3) were generated in the laboratory of K. Simons (Max Planck Institute, Dresden, Germany), and hybridomas producing anti-VSVG antibodies (TKG) were obtained from the late T. Kreis (University of Geneva, Geneva, Switzerland). Secondary antibodies labeled with Alexa fluorophores were purchased from Invitrogen, and HRP- or Cy5-conjugated secondary antibodies were obtained from Jackson ImmunoResearch Laboratories.

Cell culture

Stably transfected MDCK cells were maintained in MEM containing 7% (vol/vol) fetal bovine serum, 2 mM L-glutamine, 200 μg/ml geneticin, 4 μg/ml puromycin, and 100 μg/ml penicillin/streptomycin as previously described (Proux-Gillardeaux et al., 2005). LLC-PK1 cells stably transfected with μ1A, μ1B, or $\mu1B^{mut}$ were maintained as described previously (Fölsch et al., 1999; Sugimoto et al., 2002). To allow for polarization, cells were seeded on polycarbonate membrane filters at a density of 4×10^5 cells per 12-mm filter (for immunofluorescence) or 8×10^5 cells per 24-mm filter (for biochemical experiments; 0.4-μm pore size; Corning-Costar transwell units) and cultured for 4–6 d with changes of medium in the basolateral chamber every day.

For intracellular localization experiments, cells were seeded on Alcian blue–coated coverslips and cultured for 2–4 d. For anti–γ-adaptin staining, cells were fixed in –20°C methanol for 5 min followed by a 5-min incubation in PBS^{2+} (PBS [0.2 g/liter KCl, 0.2 g/liter KH_2PO_4, 8 g/liter NaCl, and 2.17 g/liter $Na_2HPO_4 \times 7\ H_2O$] plus 0.1 g/liter $CaCl_2$ and 0.1 g/liter $MgCl_2 \times 6\ H_2O$). Otherwise, cells were fixed in 3% (wt/vol) PFA for 15 min at RT. After fixation, cells were processed for immunofluorescence essentially as described previously (Fölsch et al., 2003).

For infection of filter-grown MDCK cells with defective adenoviruses, cultures were washed once in serum-free and calcium/magnesium-free medium, and 50–100 plaque-forming units (pfu) of the viruses was added to the apical chamber. After a 2-h incubation at 37°C, the medium was exchanged with normal growth medium. The cells were prepared for immunofluorescence analysis 2 d after infection. To express VSVG or A-VSVG, corresponding defective adenoviruses were applied to cells as described followed by a 5-h incubation at 37°C. Cells were then shifted to 39°C for 16 h, followed by a 2-h incubation at 31°C. Infection of LLC-PK1 cells was essentially done as described for MDCK cells, with the exception that cells were washed in serum-free α-MEM containing calcium/magnesium before infection in serum-free α-MEM.

For cell surface staining, the cultures were washed once with PBS^{2+} and incubated with antibodies applied to apical and basolateral sides for 7.5 min at RT. Cultures were washed three times with ice-cold PBS^{2+} and fixed in 3% PFA for 15 min at RT. Filters were then cut out and stained for immunofluorescence microscopy essentially as described.

To perform rescue experiments, 2 d after seeding, filter-grown MDCK cells were transiently transfected with LDLR-CT27 cDNA and either RFP-cb-VW or RFP-syn2-VW cDNA using Lipofectamine (Invitrogen) according to the manufacturer's protocol and incubated overnight at 37°C. Before surface staining, cells were treated with or without 0.1 mg/ml cycloheximide for 2 h at 37°C. Surface staining was performed as described. All immunofluorescence preparations were analyzed using a confocal microscope (Microsystem LSM; Carl Zeiss MicroImaging, Inc.) with a microscope (Axiovert 100; Carl Zeiss MicroImaging, Inc.) and a Plan-Apochromat 63× objective. Images were enhanced and combined using Photoshop (Adobe).

GFP-cb immunoprecipitations from MDCK cells

2 d after seeding, filter-grown MDCK cells were infected with defective adenoviruses encoding double myc-tagged syntaxin 3 or double myc-tagged syntaxin 4 (Low et al., 2006) as described. 1 d after infection, filters were washed three times in ice-cold PBS and cut out, and cells were lysed with 1.25 ml solubilization buffer (50 mM Tris-HCl, pH 8.0, 150 mM NaCl, 1% Triton X-100, and 1× protease inhibitor cocktail [Roche Pharmaceuticals]), passed four times through a 22.5-gauge needle and a 1-ml syringe, and incubated for 30 min on ice followed by a clarifying spin at 4°C in an centrifuge (13,200 rpm for 15 min; Eppendorf). The resulting supernatant was incubated with anti-GFP antibodies bound to protein A beads and rotated end-over-end overnight at 4°C. Immunoprecipitates were washed three times in lysis buffer and eluted with 100 mM glycine, pH 2.7, and 0.5% Triton X-100. The eluate was neutralized with Tris base and supplemented with SDS sample buffer, boiled for 5 min, and run on SDS-PAGE gels followed by blotting onto nitrocellulose membranes and Western blot analysis.

Immuno-EM

MDCK cells expressing GFP-cb were infected with defective adenoviruses encoding μ1A-HA or μ1B-myc as described. Infected cells were incubated at 37°C for 36 h and subsequently fixed for 1 h with 4% PFA (Electron Microscopy Sciences) and 0.25 M Hepes, pH 7.4, at RT. Cells were then left overnight in 8% PFA and 0.25 M Hepes, pH 7.4. Preparation for immunochemistry was as described previously (Fölsch et al., 2001) using rabbit anti-myc (A-14) and anti-GFP (Invitrogen) antibodies, respectively, followed by 10 and 15 nm protein A–gold, respectively (Cell Microscopy Center, Utrecht University, Netherlands). Sections were observed in an electron microscope (Tecnai 12; FEI Company), and images were captured using a charge-coupled device camera (Morada; Olympus) and saved as TIF files. Images were assembled using Photoshop without any alteration other than contrast and brightness.

Pulse-chase biotinylation

3 d after seeding, MDCK cells were infected at 14 pfu/cell as described. 16 h after infection, cells were pulse-labeled, chased, subjected to either apical or basolateral biotinylation, and harvested essentially as previously described (Anderson et al., 2005). Postlysis supernatant was spun at 100,000 *g* for 30 min (TLA 55 rotor [Beckman Coulter]; MaxE tabletop ultracentrifuge). The supernatant was then incubated with C7 antibodies coupled to protein G beads, and resulting immunoprecipitates were used for subsequent precipitation of biotinylated material essentially as previously described (Anderson et al., 2005). Samples were subjected to SDS-PAGE and autoradiography. Radioactive counts were detected using a Phosphorimager (model FLA-5100; Fujifilm). The resultant signals were analyzed using Multi Gauge Version 3 software (Fujifilm). Surface proteins were normalized against the total protein. The data are expressed as a percentage of LDLR-CT27 protein reaching each surface relative to the total amount of surface LDLR-CT27 at each time point.

Online supplemental material

Fig. S1 shows the expression of myc-tagged cellubrevin at the basolateral membrane of MDCK cells. Fig. S2 shows the intracellular localization of RFP-tagged TeNT-resistant cellubrevin or synaptobrevin 2. Fig. S3 shows the sorting of selective cargos to the basolateral or apical plasma membrane in LLC-PK1 cell lines. Fig. S4 shows the yeast two-hybrid interactions of basolateral sorting signals with adaptor complex μ-chains. Online supplemental material is available at http://www.jcb.org/cgi/content/full/jcb.200610047/DC1.

The authors thank Dr. Juan Bonifacino for providing us with μ-chain cDNAs, Dr. Ira Mellman for FcR-RFP cDNA, Dr. Thomas Weimbs (University of California, Santa Barbara, CA) for myc-tagged syntaxin 3 and 4, and Dr. Bettina Winckler (University of Virginia) for helpful comments on the manuscript. Furthermore, we thank Kimberly Zichichi for technical assistance in preparing the electron micrographs.

This work was funded by a grant from the National Institutes of Health (GM070736) to H. Fölsch and supported in part by grants from the Institut National de la Santé et de la Recherche Médicale (Avenir Program), the European Commission ("Signaling and Traffic" STREP 503229), the Association pour la Recherche sur le Cancer, the Ministère de la Recherche (ACI-BDP), and the Fondation pour la Recherche Médicale (to T. Galli). R.S. Kang was supported by the Cellular and Molecular Basis of Disease Training Program (GM8061). V. Proux-Gillardeaux was supported by a postdoctoral fellowship from the Fondation pour la Recherche Médicale.

Submitted: 10 October 2006
Accepted: 5 April 2007

References

Anderson, E., S. Maday, J. Sfakianos, M. Hull, B. Winckler, D. Sheff, H. Fölsch, and I. Mellman. 2005. Transcytosis of NgCAM in epithelial cells reflects differential signal recognition on the endocytic and secretory pathways. *J. Cell Biol.* 170:595–605.

Ang, A.L., H. Fölsch, U.M. Koivisto, M. Pypaert, and I. Mellman. 2003. The Rab8 GTPase selectively regulates AP-1B-dependent basolateral transport in polarized Madin-Darby canine kidney cells. *J. Cell Biol.* 163:339–350.

Ang, A.L., T. Taguchi, S. Francis, H. Fölsch, L.J. Murrells, M. Pypaert, G. Warren, and I. Mellman. 2004. Recycling endosomes can serve as intermediates during transport from the Golgi to the plasma membrane of MDCK cells. *J. Cell Biol.* 167:531–543.

Boehm, M., and J.S. Bonifacino. 2001. Adaptins: the final recount. *Mol. Biol. Cell.* 12:2907–2920.

Bonifacino, J.S., and L.M. Traub. 2003. Signals for sorting of transmembrane proteins to endosomes and lysosomes. *Annu. Rev. Biochem.* 72:395–447.

Bonifacino, J.S., and B.S. Glick. 2004. The mechanisms of vesicle budding and fusion. *Cell.* 116:153–166.

Bos, K., C. Wraight, and K.K. Stanley. 1993. TGN38 is maintained in the trans-Golgi network by a tyrosine-containing motif in the cytoplasmic domain. *EMBO J.* 12:2219–2228.

Brodsky, F.M., C.Y. Chen, C. Knuehl, M.C. Towler, and D.E. Wakeham. 2001. Biological basket weaving: formation and function of clathrin-coated vesicles. *Annu. Rev. Cell Dev. Biol.* 17:517–568.

Chidambaram, S., N. Mullers, K. Wiederhold, V. Haucke, and G.F. von Mollard. 2004. Specific interaction between SNAREs and epsin N-terminal homology (ENTH) domains of epsin-related proteins in trans-Golgi network to endosome transport. *J. Biol. Chem.* 279:4175–4179.

Daro, E., P. van der Sluijs, T. Galli, and I. Mellman. 1996. Rab4 and cellubrevin define different early endosome populations on the pathway of transferrin receptor recycling. *Proc. Natl. Acad. Sci. USA.* 93:9559–9564.

Fölsch, H. 2005. The building blocks for basolateral vesicles in polarized epithelial cells. *Trends Cell Biol.* 15:222–228.

Fölsch, H., H. Ohno, J.S. Bonifacino, and I. Mellman. 1999. A novel clathrin adaptor complex mediates basolateral targeting in polarized epithelial cells. *Cell.* 99:189–198.

Fölsch, H., M. Pypaert, P. Schu, and I. Mellman. 2001. Distribution and function of AP-1 clathrin adaptor complexes in polarized epithelial cells. *J. Cell Biol.* 152:595–606.

Fölsch, H., M. Pypaert, S. Maday, L. Pelletier, and I. Mellman. 2003. The AP-1A and AP-1B clathrin adaptor complexes define biochemically and functionally distinct membrane domains. *J. Cell Biol.* 163:351–362.

Galli, T., T. Chilcote, O. Mundigl, T. Binz, H. Niemann, and P. De Camilli. 1994. Tetanus toxin-mediated cleavage of cellubrevin impairs exocytosis of transferrin receptor-containing vesicles in CHO cells. *J. Cell Biol.* 125:1015–1024.

Galli, T., A. Zahraoui, V.V. Vaidyanathan, G. Raposo, J.M. Tian, M. Karin, H. Niemann, and D. Louvard. 1998. A novel tetanus neurotoxin-insensitive vesicle-associated membrane protein in SNARE complexes of the apical plasma membrane of epithelial cells. *Mol. Biol. Cell.* 9:1437–1448.

Gan, Y., T.E. McGraw, and E. Rodriguez-Boulan. 2002. The epithelial-specific adaptor AP1B mediates post-endocytic recycling to the basolateral membrane. *Nat. Cell Biol.* 4:605–609.

Gravotta, D., A. Deora, E. Perret, C. Oyanadel, A. Soza, R. Schreiner, A. Gonzalez, and E. Rodriguez-Boulan. 2007. AP1B sorts basolateral

proteins in recycling and biosynthetic routes of MDCK cells. *Proc. Natl. Acad. Sci. USA.* 104:1564–1569.

Grindstaff, K.K., C. Yeaman, N. Anandasabapathy, S.C. Hsu, E. Rodriguez-Boulan, R.H. Scheller, and W.J. Nelson. 1998. Sec6/8 complex is recruited to cell-cell contacts and specifies transport vesicle delivery to the basal-lateral membrane in epithelial cells. *Cell.* 93:731–740.

Hirst, J., S.E. Miller, M.J. Taylor, G.F. von Mollard, and M.S. Robinson. 2004. EpsinR is an adaptor for the SNARE protein Vti1b. *Mol. Biol. Cell.* 15:5593–5602.

Ikonen, E., M. Tagaya, O. Ullrich, C. Montecucco, and K. Simons. 1995. Different requirements for NSF, SNAP, and Rab proteins in apical and basolateral transport in MDCK cells. *Cell.* 81:571–580.

Jahn, R., and R.H. Scheller. 2006. SNAREs—engines for membrane fusion. *Nat. Rev. Mol. Cell Biol.* 7:631–643.

Kreitzer, G., J. Schmoranzer, S.H. Low, X. Li, Y. Gan, T. Weimbs, S.M. Simon, and E. Rodriguez-Boulan. 2003. Three-dimensional analysis of post-Golgi carrier exocytosis in epithelial cells. *Nat. Cell Biol.* 5:126–136.

Lafont, F., P. Verkade, T. Galli, C. Wimmer, D. Louvard, and K. Simons. 1999. Raft association of SNAP receptors acting in apical trafficking in Madin-Darby canine kidney cells. *Proc. Natl. Acad. Sci. USA.* 96:3734–3738.

Li, X., S.H. Low, M. Miura, and T. Weimbs. 2002. SNARE expression and localization in renal epithelial cells suggest mechanism for variability of trafficking phenotypes. *Am. J. Physiol. Renal Physiol.* 283:F1111–F1122.

Low, S.H., S.J. Chapin, T. Weimbs, L.G. Komuves, M.K. Bennett, and K.E. Mostov. 1996. Differential localization of syntaxin isoforms in polarized Madin-Darby canine kidney cells. *Mol. Biol. Cell.* 7:2007–2018.

Low, S.H., S.J. Chapin, C. Wimmer, S.W. Whiteheart, L.G. Komuves, K.E. Mostov, and T. Weimbs. 1998. The SNARE machinery is involved in apical plasma membrane trafficking in MDCK cells. *J. Cell Biol.* 141:1503–1513.

Low, S.H., A. Vasanji, J. Nanduri, M. He, N. Sharma, M. Koo, J. Drazba, and T. Weimbs. 2006. Syntaxins 3 and 4 are concentrated in separate clusters on the plasma membrane before the establishment of cell polarity. *Mol. Biol. Cell.* 17:977–989.

Martinez-Arca, S., R. Rudge, M. Vacca, G. Raposo, J. Camonis, V. Proux-Gillardeaux, L. Daviet, E. Formstecher, A. Hamburger, F. Filippini, et al. 2003. A dual mechanism controlling the localization and function of exocytic v-SNAREs. *Proc. Natl. Acad. Sci. USA.* 100:9011–9016.

Matter, K., W. Hunziker, and I. Mellman. 1992. Basolateral sorting of LDL receptor in MDCK cells: the cytoplasmic domain contains two tyrosine-dependent targeting determinants. *Cell.* 71:741–753.

Matter, K., E.M. Yamamoto, and I. Mellman. 1994. Structural requirements and sequence motifs for polarized sorting and endocytosis of LDL and Fc receptors in MDCK cells. *J. Cell Biol.* 126:991–1004.

McMahon, H.T., Y.A. Ushkaryov, L. Edelmann, E. Link, T. Binz, H. Niemann, R. Jahn, and T.C. Sudhof. 1993. Cellubrevin is a ubiquitous tetanus-toxin substrate homologous to a putative synaptic vesicle fusion protein. *Nature.* 364:346–349.

Mostov, K., T. Su, and M. ter Beest. 2003. Polarized epithelial membrane traffic: conservation and plasticity. *Nat. Cell Biol.* 5:287–293.

Munson, M., and P. Novick. 2006. The exocyst defrocked, a framework of rods revealed. *Nat. Struct. Mol. Biol.* 13:577–581.

Nakatsu, F., and H. Ohno. 2003. Adaptor protein complexes as the key regulators of protein sorting in the post-Golgi network. *Cell Struct. Funct.* 28:419–429.

Nelson, W.J. 2003. Adaptation of core mechanisms to generate cell polarity. *Nature.* 422:766–774.

Nishimura, N., H. Plutner, K. Hahn, and W.E. Balch. 2002. The delta subunit of AP-3 is required for efficient transport of VSV-G from the trans-Golgi network to the cell surface. *Proc. Natl. Acad. Sci. USA.* 99:6755–6760.

Odorizzi, G., and I.S. Trowbridge. 1997. Structural requirements for basolateral sorting of the human transferrin receptor in the biosynthetic and endocytic pathways of Madin-Darby canine kidney cells. *J. Cell Biol.* 137:1255–1264.

Peden, A.A., G.Y. Park, and R.H. Scheller. 2001. The Di-leucine motif of vesicle-associated membrane protein 4 is required for its localization and AP-1 binding. *J. Biol. Chem.* 276:49183–49187.

Proux-Gillardeaux, V., J. Gavard, T. Irinopoulou, R.M. Mege, and T. Galli. 2005. Tetanus neurotoxin-mediated cleavage of cellubrevin impairs epithelial cell migration and integrin-dependent cell adhesion. *Proc. Natl. Acad. Sci. USA.* 102:6362–6367.

Ralston, E., S. Beushausen, and T. Ploug. 1994. Expression of the synaptic vesicle proteins VAMPs/synaptobrevins 1 and 2 in non-neural tissues. *J. Biol. Chem.* 269:15403–15406.

Ravichandran, V., A. Chawla, and P.A. Roche. 1996. Identification of a novel syntaxin- and synaptobrevin/VAMP-binding protein, SNAP-23, expressed in non-neuronal tissues. *J. Biol. Chem.* 271:13300–13303.

Regazzi, R., K. Sadoul, P. Meda, R.B. Kelly, P.A. Halban, and C.B. Wollheim. 1996. Mutational analysis of VAMP domains implicated in Ca^{2+}-induced insulin exocytosis. *EMBO J.* 15:6951–6959.

Robinson, M.S., and J.S. Bonifacino. 2001. Adaptor-related proteins. *Curr. Opin. Cell Biol.* 13:444–453.

Rodriguez-Boulan, E., G. Kreitzer, and A. Musch. 2005. Organization of vesicular trafficking in epithelia. *Nat. Rev. Mol. Cell Biol.* 6:233–247.

Rossetto, O., L. Gorza, G. Schiavo, N. Schiavo, R.H. Scheller, and C. Montecucco. 1996. VAMP/synaptobrevin isoforms 1 and 2 are widely and differentially expressed in nonneuronal tissues. *J. Cell Biol.* 132:167–179.

Roush, D.L., C.J. Gottardi, H.Y. Naim, M.G. Roth, and M.J. Caplan. 1998. Tyrosine-based membrane protein sorting signals are differentially interpreted by polarized Madin-Darby canine kidney and LLC-PK1 epithelial cells. *J. Biol. Chem.* 273:26862–26869.

Schiavo, G., F. Benfenati, B. Poulain, O. Rossetto, P. Polverino de Laureto, B.R. DasGupta, and C. Montecucco. 1992. Tetanus and botulinum-B neurotoxins block neurotransmitter release by proteolytic cleavage of synaptobrevin. *Nature.* 359:832–835.

Schuck, S., and K. Simons. 2004. Polarized sorting in epithelial cells: raft clustering and the biogenesis of the apical membrane. *J. Cell Sci.* 117:5955–5964.

Sharma, N., S.H. Low, S. Misra, B. Pallavi, and T. Weimbs. 2006. Apical targeting of syntaxin 3 is essential for epithelial cell polarity. *J. Cell Biol.* 173:937–948.

Simmen, T., S. Honing, A. Icking, R. Tikkanen, and W. Hunziker. 2002. AP-4 binds basolateral signals and participates in basolateral sorting in epithelial MDCK cells. *Nat. Cell Biol.* 4:154–159.

Steegmaier, M., K.C. Lee, R. Prekeris, and R.H. Scheller. 2000. SNARE protein trafficking in polarized MDCK cells. *Traffic.* 1:553–560.

Sugimoto, H., M. Sugahara, H. Fölsch, Y. Koide, F. Nakatsu, N. Tanaka, T. Nishimura, M. Furukawa, C. Mullins, N. Nakamura, et al. 2002. Differential recognition of tyrosine-based basolateral signals by AP-1B subunit micro1B in polarized epithelial cells. *Mol. Biol. Cell.* 13:2374–2382.

ter Beest, M.B., S.J. Chapin, D. Avrahami, and K.E. Mostov. 2005. The role of syntaxins in the specificity of vesicle targeting in polarized epithelial cells. *Mol. Biol. Cell.* 16:5784–5792.

Thomas, D.C., C.B. Brewer, and M.G. Roth. 1993. Vesicular stomatitis virus glycoprotein contains a dominant cytoplasmic basolateral sorting signal critically dependent upon a tyrosine. *J. Biol. Chem.* 268:3313–3320.

Toomre, D., P. Keller, J. White, J.C. Olivo, and K. Simons. 1999. Dual-color visualization of trans-Golgi network to plasma membrane traffic along microtubules in living cells. *J. Cell Sci.* 112:21–33.

Traub, L.M. 2003. Sorting it out: AP-2 and alternate clathrin adaptors in endocytic cargo selection. *J. Cell Biol.* 163:203–208.

Yamasaki, S., A. Baumeister, T. Binz, J. Blasi, E. Link, F. Cornille, B. Roques, E.M. Fykse, T.C. Sudhof, R. Jahn, et al. 1994. Cleavage of members of the synaptobrevin/VAMP family by types D and F botulinal neurotoxins and tetanus toxin. *J. Biol. Chem.* 269:12764–12772.